Project No. 12-3382

Atomic-scale to Meso-scale Simulation Studies of Thermal Ageing and Irradiation Effects in Fe-Cr Alloys

Nuclear Energy Advanced Modeling and Simulation (NEAMS)

H. Eugene Stanley
Boston University

Collaborators
Rensselaer Polytechnic Institute

Dan Funk, Federal POC
David Pointer, Technical POC

NEUP Nuclear Energy University Programs
U.S. Department of Energy

Atomic-scale to Meso-Scale Simulation Studies of Thermal Ageing and Irradiation Effects in Fe-Cr alloys

In this project, we target at three primary objectives: (1) Molecular Dynamics (MD) code development for Fe-Cr alloys, which can be utilized to provide thermodynamic and kinetic properties as inputs in mesoscale Phase Field (PF) simulations; (2) validation and implementation of the MD code to explain thermal ageing and radiation damage; and (3) an integrated modeling platform for MD and PF simulations. These two simulation tools, MD and PF, will ultimately be merged to understand and quantify the kinetics and mechanisms of microstructure and property evolution of Fe-Cr alloys under various thermal and irradiation environments.

MD work

Modified MOLDY based MD/MMC model

The current atomic level simulations for Fe-Cr alloys will provide thermodynamic and kinetic properties as inputs in mesoscale Phase Field (PF) models and also validate and implement the molecular dynamics (MD) code to explain thermal ageing and radiation damage. We have combined an atomic level method (MD) and Metropolis Monte Carlo (MMC) approach to study the formation of secondary phases and Cr precipitates in the bulk and at grain boundaries in Fe. As well know, the accuracy of the results by these methods depends on interatomic potentials used, which describe the energy of the atomic system and the forces on each atom in the system. The interatomic potential for Fe was taken from that by Ackland and Mendelev [1], which provides reasonable description of point defects and was widely used to simulate radiation damage in Fe. The interactions for Cr and Fe-Cr were described using a two-band second moment model derived by Olsson et al [2].

A. Irradiation Enhanced Nucleation of Cr precipitates in Fe-Cr alloys

Molecular dynamics simulations were performed using the modified version of MOLDY code. The simulation cell consisted of 50 × 50 × 50 bcc unit cells (250,000 atoms), randomly distributed 10 at% and 15 at% Cr respectively. Fe atoms are randomly replaced by Cr atoms, forming substitution Cr atoms in bcc Fe. Two temperatures are considered in the present work, i.e. 300 K and 600 K, and periodic boundary conditions are imposed along the three directions. The constant number of atoms, volume and temperature (NVT) ensemble is chosen in the resent simulation with a time step of 1fs. A cascade was started by imparting the chosen kinetic energy E_p (10 keV) to one atom, i.e. the primary knock-on atom (PKA). In order to avoid channeling, the PKAs for the cascade events were initiated in the high-index direction <135>, which is located in the middle of a standard stereographic unit triangle. After the PKA was initiated, the crystal was allowed to evolve for 20 ps. The crystal containing the defects created by this cascade was then quenched to 0 K, following which it was re-equilibrated at the required temperature and a second cascade (the overlap event) was initiated. The simulation was overlapped for 10 times.

After 10 times overlap cascades, the defects formed in Fe-10 at% Cr at 300K and 600 K, and Fe-15 at% Cr at 600K were listed in Table 1, where the number of Frenkel pairs, number of Fe-Fe SIAs, number of Fe-Cr SIAs, number of Cr-Cr SIAs, size of the largest SIA cluster, fraction of Cr in all the SIAs, fraction of Cr among clustered interstitial atoms, interstitial clustered fraction and vacancy clustered fraction are presented. The number of Frenkel pairs produced is 94 at 300 K, larger than that at 600 K. Moreover, we also observed that the number of Fe-Cr SIAs and Cr-Cr SIAs, and fraction of Cr among clustered interstitial atoms were larger for the Fe-15 at% Cr alloy than the Fe-10 at% Cr

alloy. It suggests that the concentration of Cr will affect the production of defects, especially related with Cr defects.

At the end of cascade overlap, the MMC simulations are performed within the NVT ensemble, and the required temperatures remain the same as the MD simulations. Two types of trials are considered: (i) random displacements of all atoms from their current positions, by which the lattice relaxation and vibration entropy are taken into account; (ii) randomly swapping of lattice sites between atoms of different kinds [3]. The new configuration is accepted if it leads to energy decrease or with a probability evaluated from the relevant Boltzmann distribution. The configurations reported here were correspond to averaging the atomic positions over the last of 10^5 macrosteps. The criterion used to establish the steady-state is based on the convergence of the total energy of the system. The final configuration may need at least 5×10^5 macrosteps. The positions of Cr atoms and vacancies in the box after 10^5 MMC steps are shown in Figure. 1 (a)-(c). As can be seen, a large number of vacancies are formed at the core of the cascades, and these vacancies enhance the nucleation of Cr precipitates. This is first time to demonstrate that the Cr precipitates prefer to form at the cores of displacement cascades, where the vacancy-rich regions are formed.

B. Precipitates of Cr at Grain Boundaries in α-Fe

In the present simulations, a modified version of the MOLDY computer code is employed. Two symmetric title GBs are studied in this work, both with a common <101> tilt axis. The two GBs are Σ3 {112} and Σ73 {661}, which atomic structures are shown in Figures. 2(a) and (b). The block sizes of Σ3 and Σ73b are 84.10Å×140.00Å×80.74Å with 80,240 Fe atoms and 103.50Å×142.00Å×80.76Å with 100,440 Fe atoms, respectively. Periodic boundary conditions are imposed along the x and z directions, but fixed boundary conditions are applied along the y direction, where the representations of x, y and z directions in the two GB models are indicated in Figure. 1. In Figure. 1, the region F consists of six atomic planes in which atoms are rigidly fixed in their original position, whereas the atoms in the region T is used to control the temperature by performing a velocity rescaling on atoms every 200 time steps according to the difference between the current temperature and the desired temperature. The top and bottom parts are vacuum lays with 15 angstrom.

The NVT (constant number of atoms, volume and temperature) ensemble is chosen in the present simulations with a time step of 1 fs. Initially the simulation cell is quenched to 0 K at constant pressure with molecular statics (MS) approach. Vacancies and Cr atoms are inserted at random positions within the stressed region near the GB core at local Cr concentrations of 5 %, 10 % and 15 %, and vacancy ratios of 0 %, 5 %, 10 % and 15 %, which are the ratios of the number of Cr atoms and vacancies to the Fe atoms within the considered stressed region (6800 and 12120 Fe atoms for Σ3 and Σ73b GBs, respectively). After Cr and vacancy insertion, the cell is again quenched to 0 K to obtain the minimum energy configuration, followed by a temperature rescaling to the required temperature and relaxation for 1 ns. Three temperatures of 300 K, 600K and 1000 K are considered.

For Σ3, the accumulation and segregation of Cr atoms and the evolution of the GB configurations depend on local vacancy concentration, Cr concentration and temperature. At the early stage, the strong attraction of Cr with the GB core provides a pathway for Cr atoms to quickly accumulate within the GB core. It is of interest to find that high vacancy concentrations enhance the long-distance migration of Cr, thus leading to the formation of the large Cr precipitates (α' phases) and voids near the GB core, as shown in Figure. 3. The surfaces of voids are found to be largely depleted by Cr, which is strongly dependent on vacancy concentration. With the increase of Cr concentration, the size and number of Cr precipitates increase, and the strong segregation of Cr at the GB is observed. Also, the number and size of Cr precipitates significantly increase with increasing the temperatures from 300 K to 1000 K. The

accumulation and segregation of Cr atoms at the GB lead to significant deformation of the GB structure and the formation of several GB steps, causing the displacement and broadening of the GB interface. However, it should be noted that the simulation time is about 10 ns, which may be not enough to study the evolution of these small precipitates. As for Σ73b GB, the MD simulations have not been completed.

C. Precipitates of Cr at Grain Boundaries in α-Fe, as Revealed by MMC Approach

In order to extend time scale, we have further explored the segregation of Cr at MMC method. The Σ3 GB was prepared considering mirror symmetry for a bi-crystal, which contains two symmetric grain boundaries so that a periodic condition can be applied along the y direction. Once the global energy minimum is identified we apply rigid-body translations of the grains and perform the full relaxation of the crystal to find minimum energy configuration of the GB (so called γ-surface). The selected shift and optimal spacing were then used to construct 3D periodic crystals with 81600 Fe atoms, where the geometrical size was 29.4×49.1×28.3 (a_0× a_0× a_0). Vacancies and Cr atoms are inserted at random positions within the stressed region near the GB cores at the local Cr concentrations of 5 % and 10 %, and a vacancy ratio of 10 % , which are the ratios of the number of Cr atoms and vacancies to the Fe atoms within the considered stressed region (16320 Fe atoms). Also, we randomly distribute 10% Cr in the whole simulation cell for comparison, where the ratio is the number of Cr atoms to all the Fe atoms of 81600. These configurations were relaxed and quenched using molecular dynamics method, as described above. Similar to the previous MD simulations, the strong attraction of Cr with the GB core provides a pathway for Cr atoms to quickly accumulate within the GB cores at this early stage. These configurations are used as initial inputs for MMC simulations. For MMC simulations, periodic boundary conditions are imposed along the x, y and z directions within the NPT ensemble. The positions of Cr atoms and vacancies in the bi-crystals GB after 3×10^5 MMC steps are displaced in Figure. 4. It can be clearly seen that the vacancies are mainly accumulated near the core of GBs, forming large voids. However, Cr atoms are randomly distributed in the whole cell for both cases considered. These results may be correlated the binding energiers of Cr atoms to Σ3 GB, which needs to be further explored. In order to comparison, a bi-crystal of Σ11 will be calculated.

Table 1. Comparison among defects formed in 10 keV cascades in Fe-10 at% Cr at 300 K and 600 K, and Fe-15 at% Cr at 600K, after 10 times overlap cascades.

	Fe-10 at% Cr at 300K	Fe-10 at% Cr at 600K	Fe-15 at% Cr at 600K
Number of Frenkel pairs	94	74	73
Number of Fe-Fe SIAs	7	2	5
Number of Fe-Cr SIAs	1	2	3
Number of Cr-Cr SIAs	0	0	1
Size of largest SIA cluster	5	8	6
Fraction of Cr in all SIAs (%)	17	23	22
Fraction of Cr among clustered interstitial atoms (%)	19	21	32
Interstitial clustered fraction (%)	39	45	26
Vacancy clustered fraction (%)	65	69	53

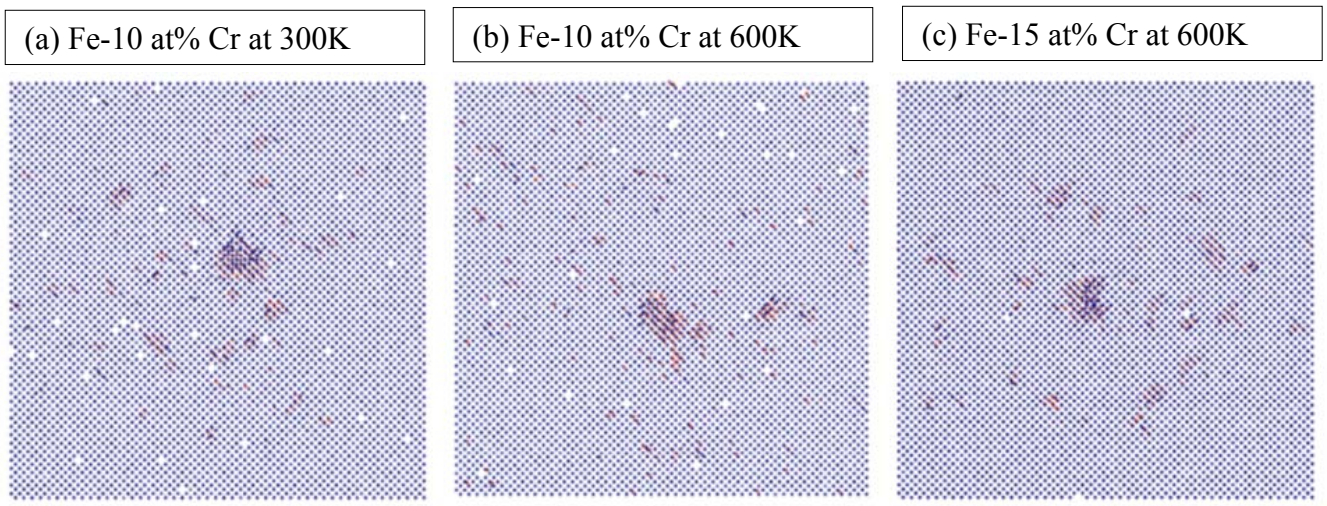

Figure. 1: *Positions of Cr atoms and vacancies in the box after 105 MMC steps, (a) Fe-10 at% Cr at 300 K, (b) Fe-10 at% Cr at 600 K, (c) Fe-15 at% Cr at 600 K. The Cr- atoms are represented in blue while the vacancies are represented in red.*

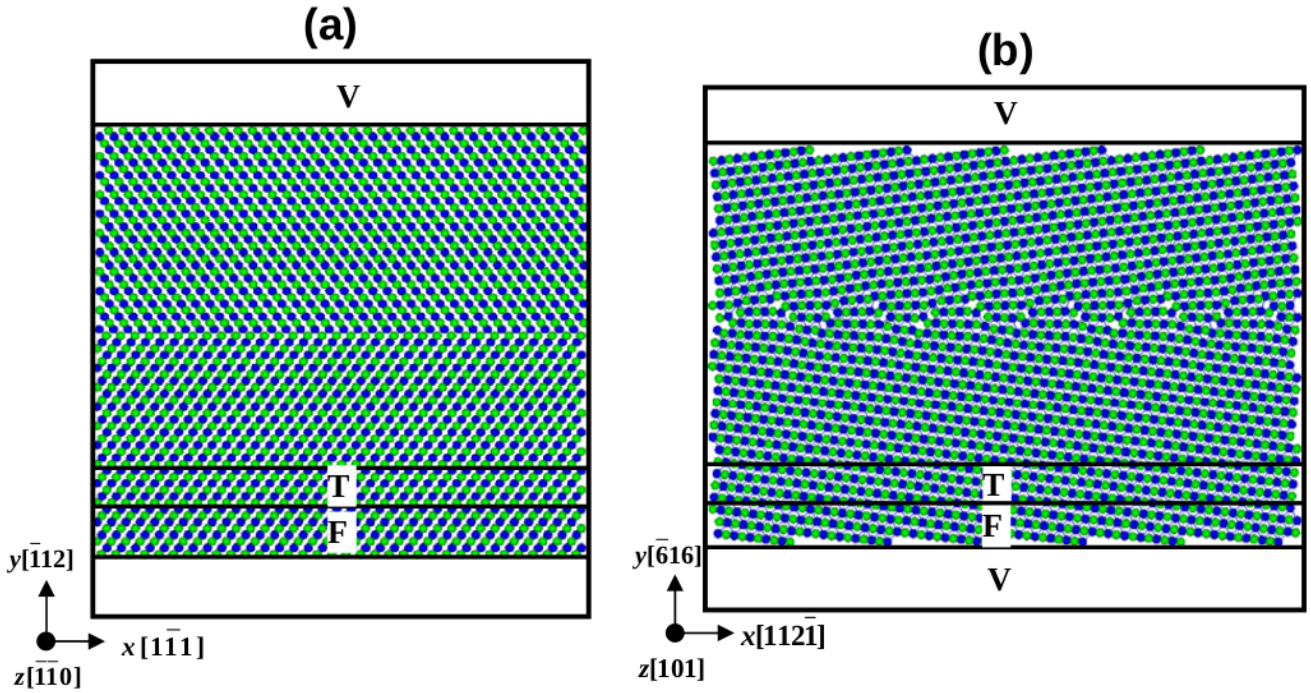

Figure. 2: *Atomic structures and model geometry used in GB simulations in α-Fe for Σ3{112} (a) and Σ73{661} (b), where green and blue spheres correspond to the two adjacent atom layers along*

the tilt axis. The representations of V, F and T are described in text in detail.

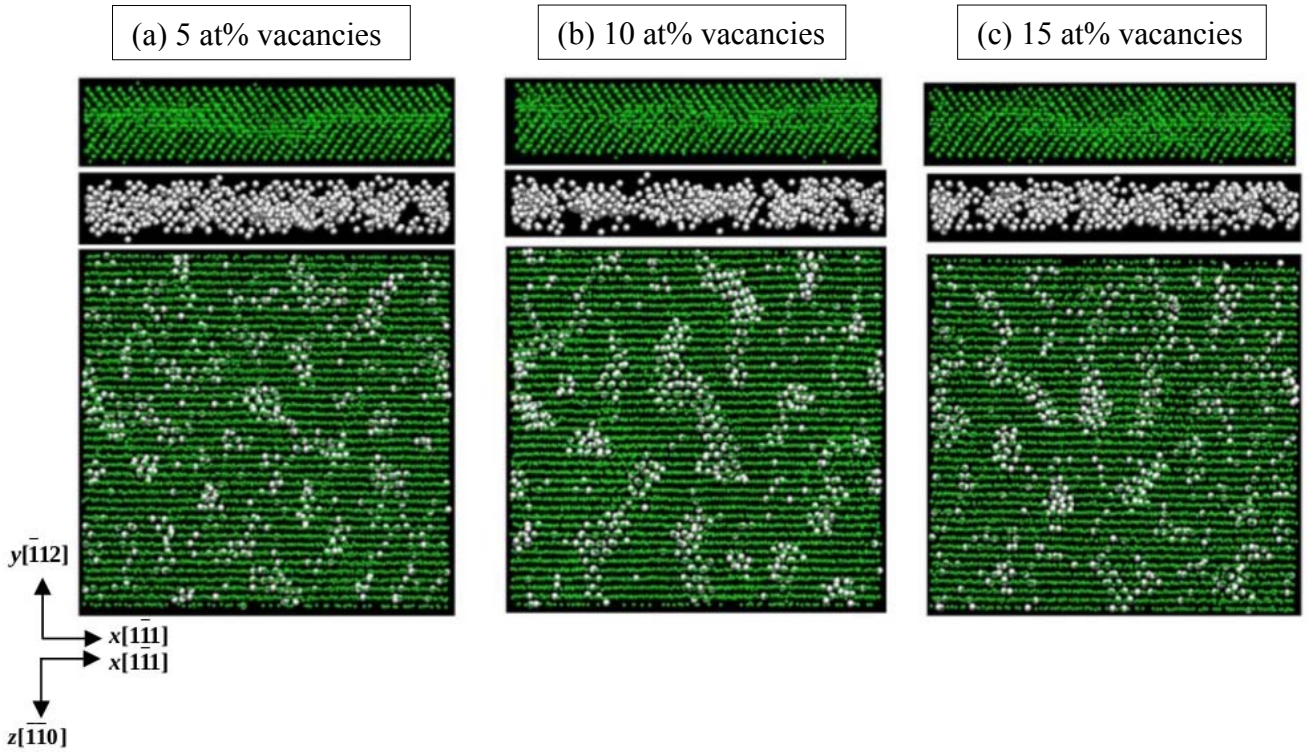

Figure. 3: *Cr distribution and configuration of Σ3 core in α-Fe with 10 at% Cr, after relaxation for 1 ns at 1000 K: (a) with 5% vacancies (b) with 10% vacancies (c) with 15% vacancies, where in each case the upper two images show a view normal to the tilt axis and the lower image shows a view normal to the GB plane. The Cr-atoms are represented by gray spheres, while the Fe-atoms are represented by green spheres.*

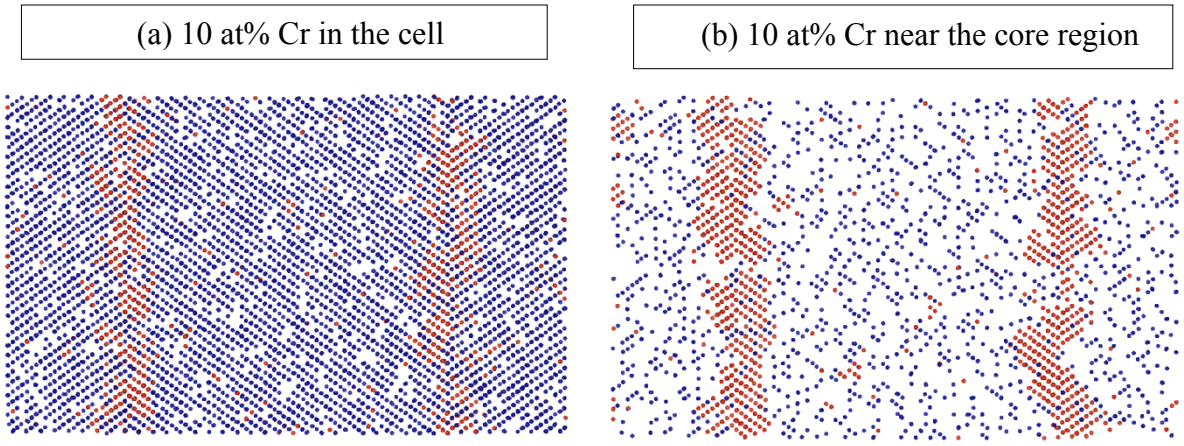

Figure. 4: *Positions of Cr atoms and vacancies in the bi-crystal after 3×10^5 MMC steps, with 10 at% vacancies near the GB core; (a) 10 at% Cr in the whole cell and (b) 10 at% Cr near the core region of GB. The Cr- atoms are represented by blue spheres, while the vacancies are represented by red spheres.*

We have continued the simulations of irradiation enhanced nucleation of Cr precipitates in Fe-Cr alloys by combining molecular dynamics (MD) method and Metropolis Monte Carlo (MMC) approach. As described before in our quarterly reports, the MMC simulations are performed within the NVT ensemble at the end of cascade overlap, and the required temperatures remain the same as the MD simulations. Two types of trials are considered: (i) random displacements of all atoms from their current positions, by which the lattice relaxation and vibration entropy are taken into account; (ii) randomly swapping of lattice sites between atoms of different kinds. The new configuration is accepted if it leads to energy decrease or with a probability evaluated from the relevant Boltzmann distribution. The configurations reported here were correspond to averaging the atomic positions over the last of 10^5 macro steps. The criterion used to establish the steady-state is based on the convergence of the total energy of the system. The final configuration may need at least 5×10^5 macro steps. We have used so called short range order (SRO) parameter to further analyze the nucleation of Cr precipitates under irradiation.

The thermodynamically equilibrium configurations of Fe-Cr alloys are simulated using MMC approach, with 2×10^5 MMC steps. The evolution of the first shell SRO parameter, the second shell SRO parameter and the SRO_{12} (defined as the coordination number-weighted average of the SRO parameters for the first and second neighbor shells) as a function of the MMC steps is shown in Figs. 5(a) – (c), respectively. All the SRO parameters increase with the increase of MMC steps. Initially, the SOR parameters show a fast increases, but become slow after $5x10^4$ MMC steps. The SRO parameters become positive after a few hundred MMC steps, correlating to the formation of Cr clusters. In Fe-15 at% Cr system, the SRO parameters are higher than in Fe-10 at% Cr, and the increasing rate of the SRO parameters is faster in Fe-15 at% Cr, compared with Fe- 10 at% Cr. In the Fe-10 at% Cr system, the SRO parameters are higher at 300 K than those at 600 K, and the increasing rate of the SRO parameters is faster at 300 K compared with that at 600 K. These results indicate that the decrease of temperature somewhat increases the probability of Cr clusters because of low binding energies of Cr atoms to a cluster, leading to Cr atoms dissociation from the cluster at high temperatures.

In addition, we initiate the work to develop the phase field model for studying the nucleation and growth of Cr precipitates in Fe-Cr systems. The phase model will read the thermodynamic and kinetic properties and the configurations of defects and interfaces calculated by the atomistic simulations, employ the Cahn-Hilliard equations to describe the diffusion of atoms and defects, instead of the stochastic events and directional and fast migrations employed by the lattice Boltzmann method and the first Passage Monte Carlo method. The model allows for the simulation of nucleation and growth of Cr precipitates and defect segregation at internal boundaries and surfaces, and large defects and elastic-plastic deformation on microstructure evolution. Also, the PFM will be employed to establish predictive models linking the simulated microstructures with experiments.

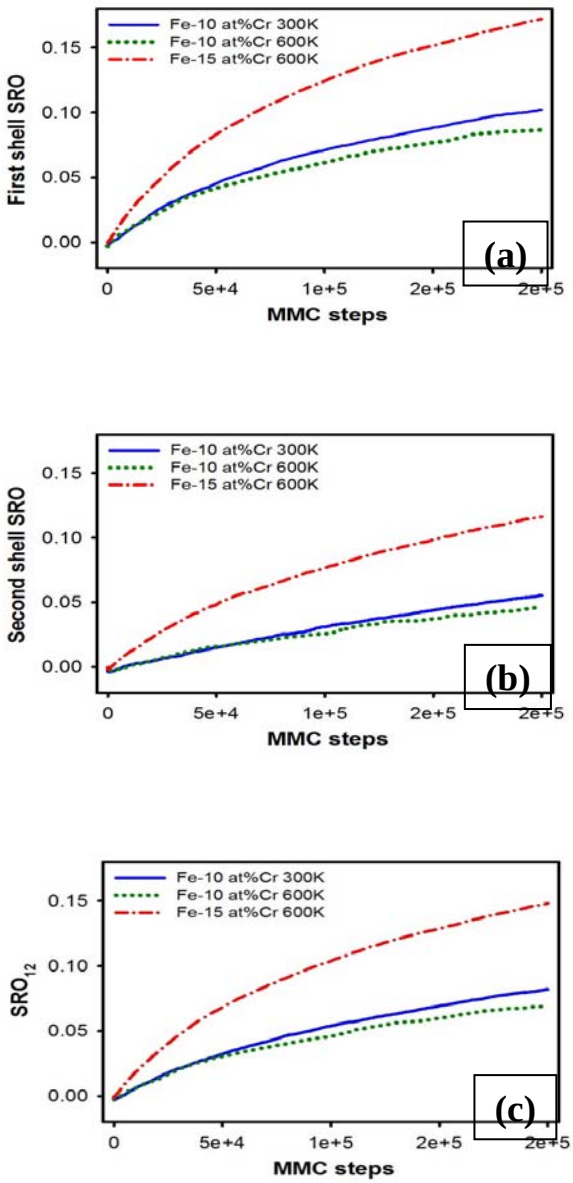

Figure. 5: *The variation of ordering as functions of Metropolis Monte Carlo simulation time-steps in Fe-Cr alloys: (a) first shell SRO parameter, (b) second shell SRO parameter, and (c) the coordination number-weighted average of the first and second SRO parameters.*

LAMMPS based MD model

After considering several different MD codes (including Gromacs, MDCASK, LAMMPS, as well as writing our own code from scratch), we have decided that the best and most efficient approach is to use LAMMPS. This is a very popular open source MD simulator, used by many scientific groups around the world, and is currently maintained by Sandia National Laboratories, a US Department of Energy laboratory. The acronym LAMMPS stands for Large-scale Atomic/Molecular Massively Parallel Simulator and as such one if its primary goals is to be fast and parallelized. The code is well-documented, regularly updated, and easy to adapt or extend.

Several models for FeCr are available, but as of yet there is not one particular model that is truly

outstanding. In Bonny *et al.*, J. Nucl. Mat. **385**, 268 (2009) [4] several state-of-the-art models for FeCr are listed, including the concentration-dependent model (CDM) and the two-band method (2BM). It is not too difficult to implement a new model into LAMMPS, but currently we are working with CDM for which an implementation was already available. We plan to include more models in the future as a comparison, as well as possibly develop new MD models ourselves.

The CDM model by Caro et al [5] has been shown to correctly predict the mixing enthalpy as well as the correct short-range order (Cr atoms prefer to be around Fe atoms below 10%Cr, but precipitate around 15%Cr). To test our implementation of CDM in LAMMPS, we have calculated the melting line as a function of Cr content. We first construct an elongated box such as that in Figure. 6 that consists of 50% liquid and 50% bcc crystal. We then run the simulation at different temperatures to determine when the system fully crystallizes and when it fully liquefies. The temperature that lies right between these two extremes is the melting temperature, and we have plotted these in Figure. 7 on top of the "official" phase diagram of FeCr according to the CALPHAD database. Even though the model has been developed for simulations at temperatures around 700 K, it still produces a decent prediction of the melting line which occurs at far higher temperatures.

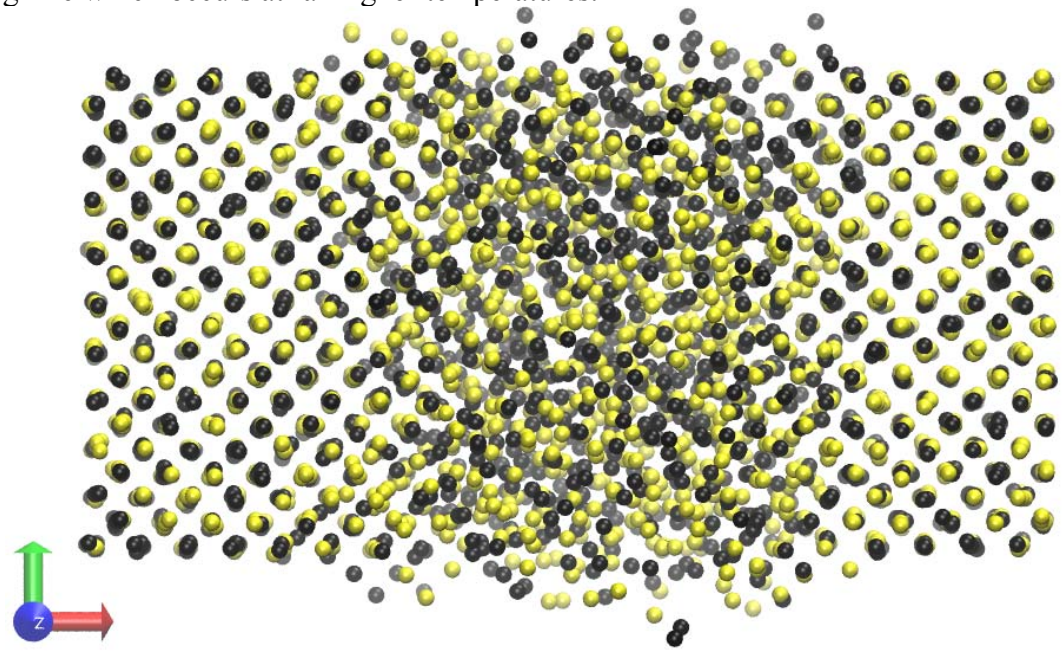

Figure. 6: Determination of the melting temperature of Fe-Cr with 50% Cr by simulating an elongated box that is half crystal / half liquid at a particular temperature T. The box will start to fully crystallize if T is below the melting temperature, and fully liquefy if T lies above the melting temperature. Here black is Fe and yellow is Cr.

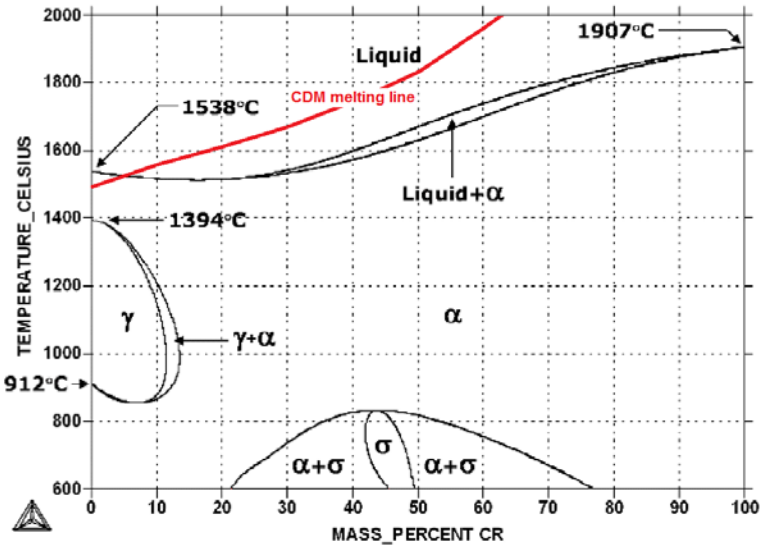

Figure. 7: Phase diagram of FeCr according to CALPHAD, including the melting temperatures predicted by the CDM model (red curve). CDM gives a reasonable value for low Cr content, but deviates more and more from the CALPHAD value as the Cr content is increased. At 100% Cr content (pure Cr) the CDM predicts a melting temperature of about 2780 °C.

The phase field simulations will require calculation of the free energy involved with grain boundaries, and it is therefore important to be able to produce such grains in the MD simulations. Now that we know the melting temperatures, it is easy to create any desired configuration of grains, in any size and shape. In Figure. 8 we present one simple example of a grain boundary that consists of two bcc lattices with a relative angle of 60° .

The next stage of this project will focus on the implementation of radiation effects. In Figure. 9 we show one of our first results: the effect of a 10 keV neutron hitting one of the Fe atoms.

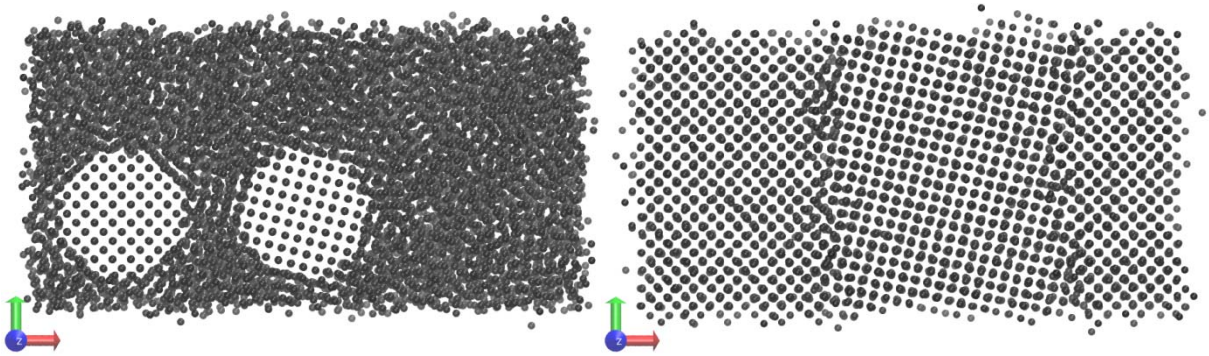

Figure. 8: Any type of grain boundary can be created by starting with two or more crystal nuclei within a liquid (left image). When the temperature is kept slightly below the melting temperature, the crystal nuclei grow and form the desired configuration (right image).

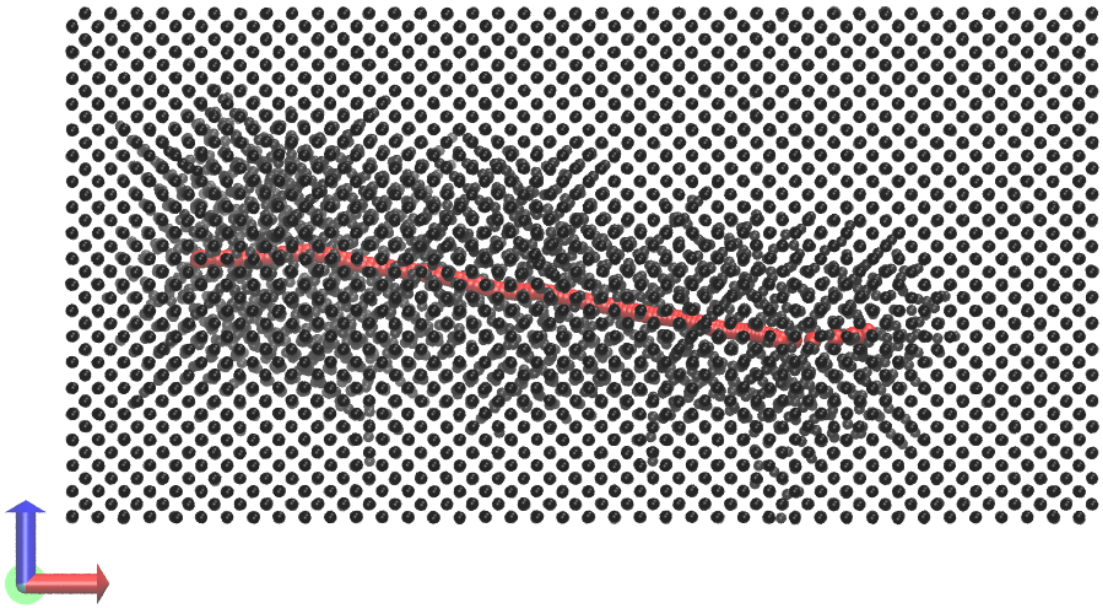

Figure. 9: Simulation of exposure to radiation. Here we simulated the effect of a 10 keV neutron hitting a Fe atom dead on. The trajectory of the first atom that got hit (often referred to as the Primary Knock-on Atom) is indicated in red. The PKA hits other atoms, which leads to a cascade of collisions. As is evident from this picture, the volume near the trajectory of the PKA becomes essentially liquefied. When the system is at a temperature far below the melting temperature, the crystal quickly recrystallizes.

To expand our simulation to tasks involving millions of atoms, our LAMMPS code are designed to suit running in parallel on a large number of processors and has also been extended by us to run on graphical processor units (GPUs). More scripts are written in order to glue LAMMPS executable file and phase field code together and make the whole simulation more user-friendly. The main scripts are:

- A script to easily generate large systems of a given size, with an arbitrary ratio of Fe:Cr atoms, and with a given number of grains. The user simply indicates for each grain the approximate location of its Voronoi center (the "seed"), as well as the lattice orientation of each grain. After the creation of the requested system, LAMMPS will automatically do an energy minimization, followed by a short molecular dynamics run to equilibrate the system. An example of the output is shown in Figure. 10.
- A script that simulates the irradiation of the system by neutron bombardment. As a minimum, this script will require the energy of the incoming radiation. However, we are planning to make this script more
- Several scripts for analysis and post-processing of the LAMMPS output, such as structural analysis and scripts that help with the visualization. For the visualization we mainly use VMD, an open-source molecular visualization program developed by the University of Illinois at Urbana-Champaign.

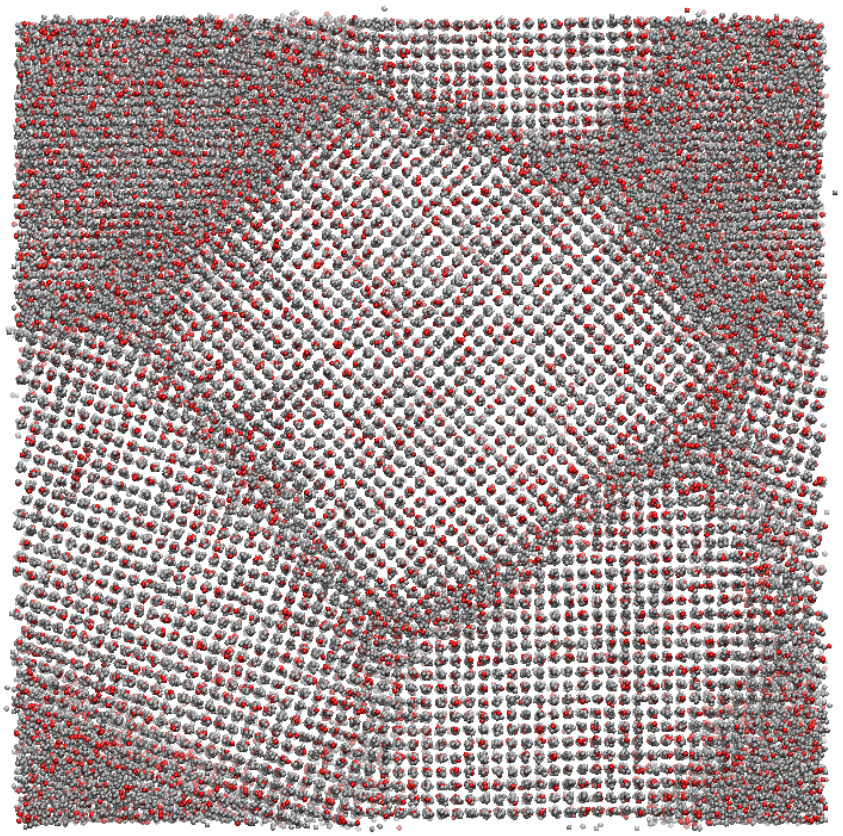

Figure. 10: Using the new python scripts it is easy to construct a large FeCr system with several grains. Shown here is a cubic system of approx. 12x12x12 nm consisting of over 128,000 atoms, with 80% Fe (gray) and 20% Cr (red). This particular system (with periodic boundaries) has 4 grains, each with a different lattice orientation.

- Previously, we were only able to run simulations by manually creating a LAMMPS input file, and then providing this file to LAMMPS. Even though this is the standard method of working with LAMMPS, it is difficult to write an input file that works like a script. For example, it is possible to work with variables and loops inside a LAMMPS input file, but this is far from trivial.
- Fortunately, it is possible to call LAMMPS commands directly from within a Python script. Python is a very popular scripting language with a straightforward syntax, and is the best scripting language to use for this project. In the last few months we have successfully created the LAMMPS/Python coupling by building LAMMPS as a shared library and then importing it from within a Python script. This coupling with Python has made the LAMMPS installation more complex, but will significantly reduce the required effort for further development of the scripts.
- In the next few months we will finalize these above-mentioned scripts, with the main focus on the script necessary
- A script to convert the LAMMPS output into input files for the phase field simulation. This work is being done in close cooperation with the RPI group, and will have our main focus the next few months.
- Several scripts for analysis and post-processing of the LAMMPS output, such as structural analysis and scripts that help with the visualization. For the visualization we mainly use VMD, an open-source molecular visualization program developed by the University of Illinois at

Urbana-Champaign.

- Scripts to connect the molecular dynamics stage with the phase field stage, i.e. the script that converts the LAMMPS output into input files for the phase field simulation sophisticatedly and allows the user to provide a histogram to the script that contains the probability distribution of the neutron energy. To make the simulation more efficient, we dynamically adjust the time step. When one or more atoms move at very high speed (such as right after the neutron has collided with an atom) the time step needs to be made small enough to produce the correct trajectories. However, after the speed of these atoms has been significantly reduced through collisions, the time step is automatically increased to allow the simulation to speed up.

Phase field work

We took use of phase field method to study the nucleus growth process in Fe-Cr solution, whose free energy function was provided by A. Caro and co-workers in 2007[6].

First, we have developed our own C++ code to simulate the Fe‐Cr evolution and get the equilibrium profile at 1×1×216 grids via the finite element method (FEM) and temporal integration. According to the material kinetics theory, Cr equilibrium concentration in Cr precipitate and Cr solubility in Fe-Cr solution can be calculated by applying common tangent method to the free energy function. Our simulation results, as shown in Figure-11, turn out to match the theoretical values exactly. In addition, we find out that Cr precipitate has very thin boundary layer, just four-grid thick. We will call nucleus with such thin layer “precipitate-like”.

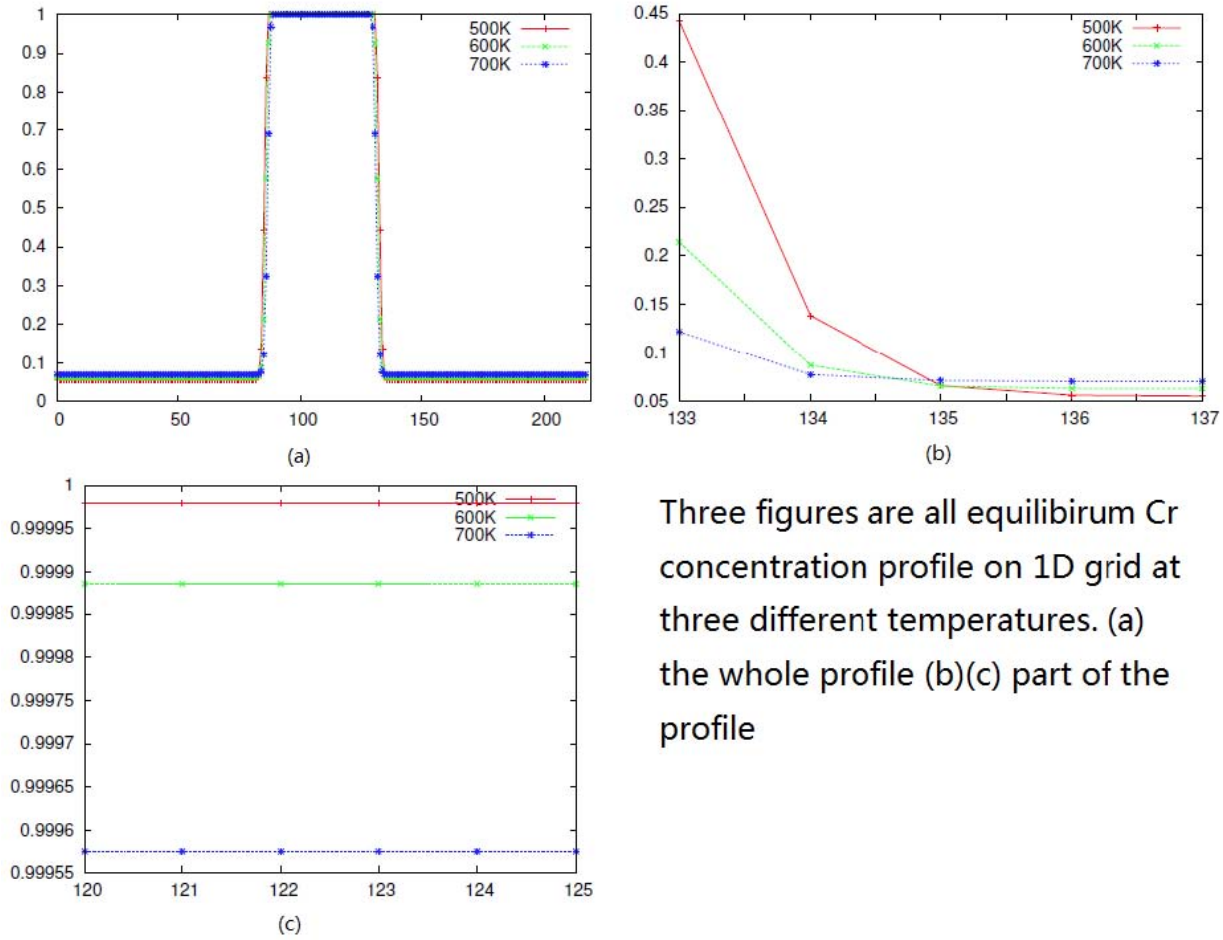

Figure. 11: Cr concentration profile at equilibrium state on 1D grid at different temperatures.

We also took use of Multiphysics Object - Oriented Simulation Environment (MOOSE) framework[8], developed by Idaho National Laboratory, to implement phase field simulation on Fe-Cr system. As it is mentioned in 2014 publication by Y. Li et al[7], there exist both classical and non-classical nucleation in Fe - Cr solution. However, the latter process, whose Cr concentration in stable nucleus is lower than Cr equilibrium concentration in Cr precipitate, has not been observed yet via MOOSE. Instead, we have observed the classical nucleation process, during which Cr concentration in nucleus grows into Cr equilibrium concentration in Cr precipitate, in our simulation. Moreover, from cases shown in Fig - 12, we may conclude that classical nucleation is more likely to occur for "precipitate-like", large size and high Cr concentration nucleus. In contrast, "Gaussian-like" (with thick boundary layer like Gaussian-function-shape concentration profile), small size and low Cr concentration nucleus tends to dissolve in Fe-Cr solution.

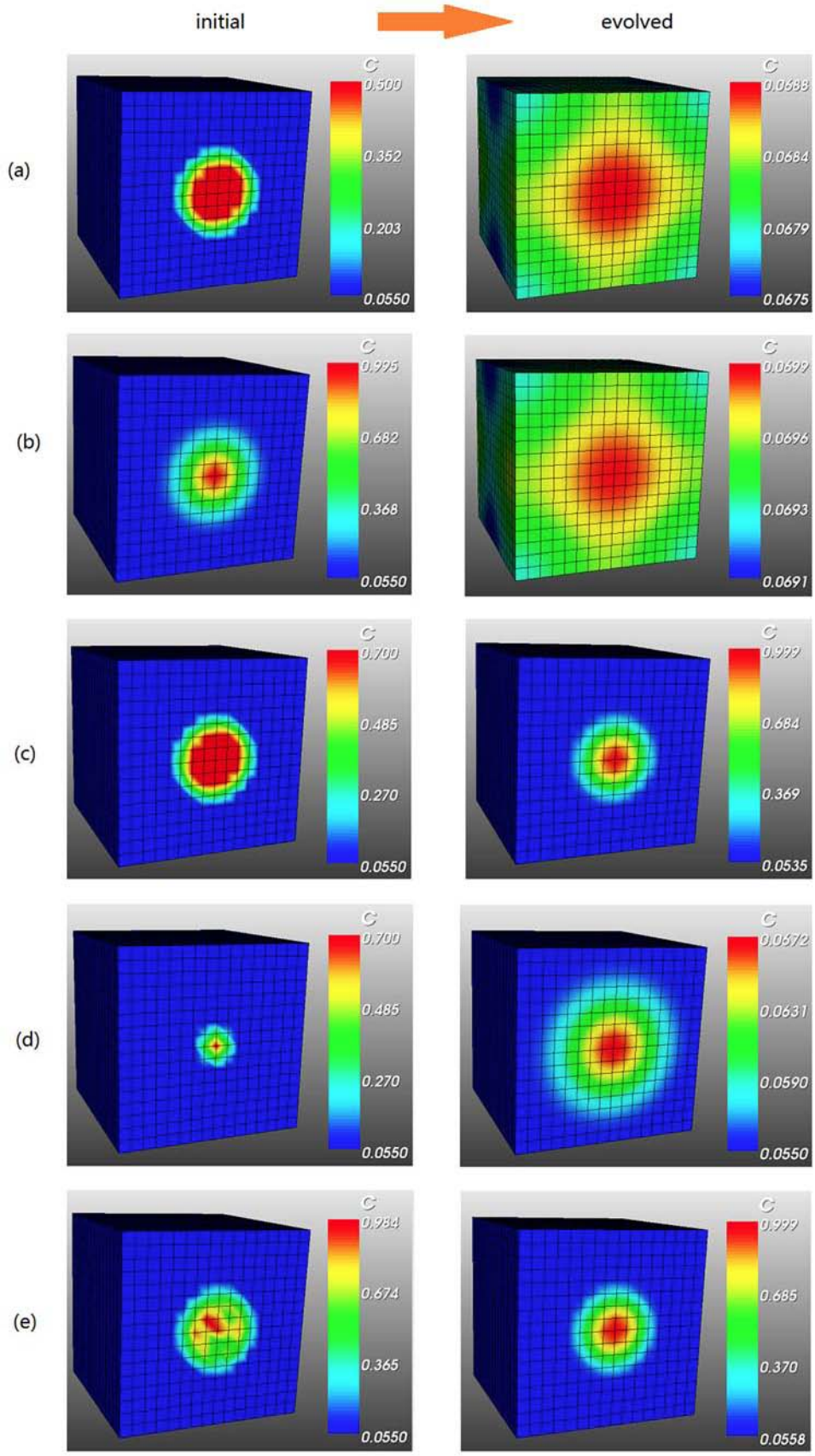

Figure. 12: (a)Precipitate-like initial nucleus dissolves in Fe-Cr solution, initial Cr concentration is 0.5 inside (b)Gaussian-like initial nucleus dissolves in Fe-Cr solution, maximum initial Cr concentration is

0.995 (c) Precipitate-like initial nucleus grows into classical nucleus, initial Cr concentration is 0.7 inside (d) Small size precipitate-like initial nucleus dissolves in Fe-Cr solution, initial Cr concentration is 0.7 inside (e) Precipitate-like initial nucleus grows into classical nucleus, initial Cr concentration is 0.69±0.3 inside

MD-Phase field bridging work

Our ultimate goal is to connect MD simulations with phase field (PF) simulations, i.e., to develop code that uses MD output to determine the best PF input. At the core of the PF simulation lies the Cahn-Hilliard equation [7],

$$\frac{\partial c}{\partial t} = \nabla \cdot \left(M \nabla \left(\frac{N_A}{\Omega_0} \frac{\partial f}{\partial c} - \kappa \nabla^2 c \right) \right)$$

where N_A is Avogadro's number, $\Omega_0 = 1.4087 \times 10^{-5}$ m^3/mol the molar volume of bcc Fe, M the mobility (related to diffusivity), and κ the interfacial energy coefficient. Running a PF simulation is equivalent to solving for $c(\mathbf{x},t)$, which is the concentration of Cr atoms at position $\mathbf{x}$ and time t.

Before we can solve the Cahn-Hilliard equation we need to have a value for all its parameters, as well as an explicit expression for the free energy density $f(c,T)$ – a function of the Cr concentration c and the temperature T. An expression for $f(c,T)$ was first presented by Schwen *et al.* [9] and has been reproduced by our group, as indicated in our previous report. This leaves us with determining the parameters M and κ.

The interfacial free energy can be estimated via Monte Carlo simulations in the variance-constrained-semi-grand-canonical (VC-SGC) ensemble and direct thermodynamic integration across phase boundaries, as shown by Sadigh and Erhart [12]. In general, the interfacial energy is anisotropic and the coefficient κ is a tensor [10], but for simplicity we may assume that is approximately isotropic and that κ is a scalar. By fitting the results of Sadigh and Erhart, it is then possible to obtain κ as a function of temperature [12].

The mobility M can be obtained via the diffusivity D, using the relation $M = D\Omega_0/RT$ where R is the gas constant and T the temperature [10]. However, it is not a trivial task to obtain the diffusivity from MD simulations, because the atoms move at an incredibly slow pace through the lattice. One solution to this problem is to assume that M is constant, and then redefine the time t in the Cahn-Hilliard equation [10]. The equation can then be solved, but the results are no longer quantitative but merely qualitative, i.e., one can perform an accurate analysis of all phenomena involved, but it is impossible to produce any numerical predictions.

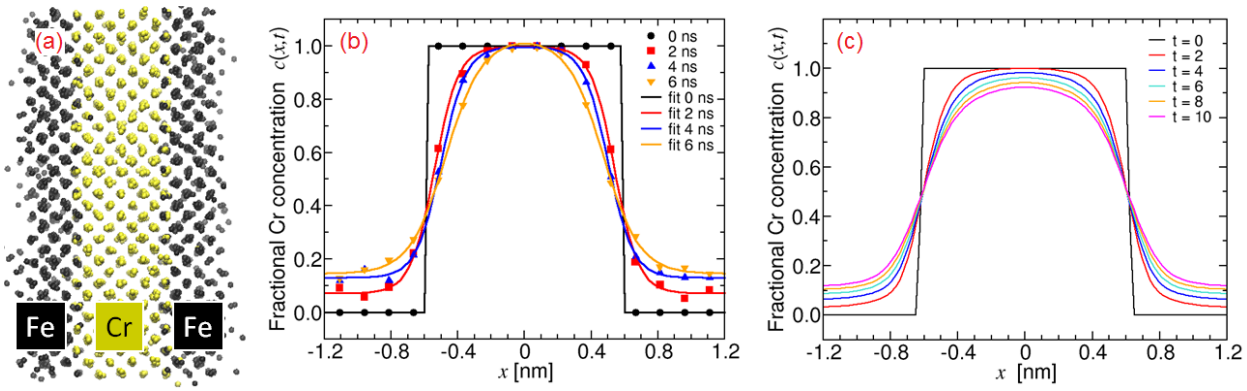

Figure. 13: (a) A slab of 100% Cr within a matrix of 100% Fe is an efficient configuration to study diffusive properties of FeCr, because of its large gradient dc/dx. (b) Evolution of the configuration of panel (a) simulated using Molecular Dynamics. The configuration has 4096 atoms with 4% Frenkel defects (i.e., 4% of the atoms have been moved from the lattice to a randomly chosen interstitial location). The simulation is kept at a constant temperature T = 2100 K and kept at a fixed size. The average pressure is about –25 kbar. (c) The same configuration also at T = 2100 K but simulated using Phase Field, using parameters M = 1.0 and κ= 0.8.

In order to perform PF simulations that allow for numerical predictions, it is therefore necessary to speed up diffusion in MD simulations. There are several ways to do this, including simulating at high temperatures and negative pressures. By performing many simulations at different T and P, one may then extrapolate the results to lower T and positive P. A large increase in diffusivity can be obtained by introducing defects in the lattice, such as vacancies, interstitial atoms, Frenkel defects (a vacancy plus an interstitial atom), grain boundaries, etc. Finally, we can speed up our analysis by considering a large gradient dc/dx which does not increase the diffusion but does increase the flux of atoms.

An ideal system to study is therefore a slab of Cr as shown in Figure. 14a. The evolution of such a system using MD is shown in Figure. 13b. The exact same configuration can also be studied using PF, and this produces a similar result (see Figure. 13c). To construct a PF simulation that describes the exactly same system, we need to adjust M and κ such that both figures are exactly the same. To facilitate this comparison, we introduce a simple formula (based on the logistic formula) to estimate the shape of $c(x)$ for both MD and PF,

$$c(x) \approx \frac{A}{1+\exp[-(x+x_I)/\sigma]} - \frac{A}{1+\exp[-(x-x_I)/\sigma]} + c_b$$

with fitting parameters A, x_I, σ, and c_b. This fit works surprisingly well for both MD and PF. Using this mapping we will be able to finally connect Molecular Dynamics to Phase Field: given the temperature, pressure, percentage of Frenkel defects, and the initial configuration, we will be able to estimate the mobility M and the interfacial energy coefficient κ required to run an equivalent Phase Field simulation.

Preliminary MD simulations also indicate that the mobility might strongly depend on the Cr concentration as well (see Figure. 14).

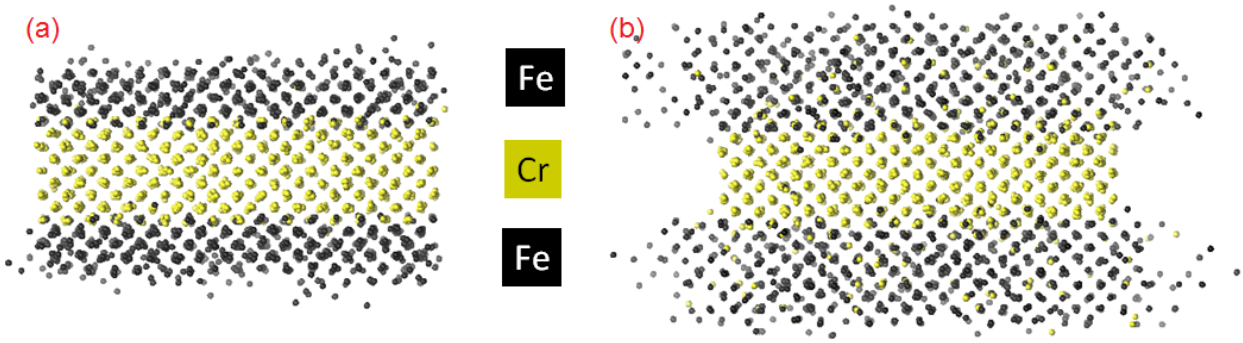

Figure. 14. Snapshots of a Molecular Dynamics of the slab from Figure.13a. The snapshot in panel (a) was taken after 0.003 ps while (b) is at 0.27 ps. From these snapshots it is clear that the diffusion of both Fe and Cr is much larger in the Fe matrix (black area) than it is in the Cr matrix (yellow area). This possibly implies that the mobility depends on the Cr concentration.

Figure.14 shows that the atoms travel further within the region where the concentration of Cr is low. To quantify the difference in mobility, we have focused on the mean squared displacement of the atoms, i.e. $\langle \Delta r \rangle^2$ as a function of time t. For ordinary diffusion, as time $t \to \infty$, one would expect the mean squared displacement to be proportional to time: $\langle \Delta r \rangle^2 = 6Dt$ (in three dimensions), with D the diffusion coefficient. Figure.15, however, shows clearly that we do not recover this relation (indicated by the brown dashed line), and that we consistently find the mean squared displacement $\langle \Delta r \rangle^2$ to be proportional to t^b instead (where b is the slope of the straight line when we plot $\log\langle \Delta r \rangle^2$ versus $\log t$.).

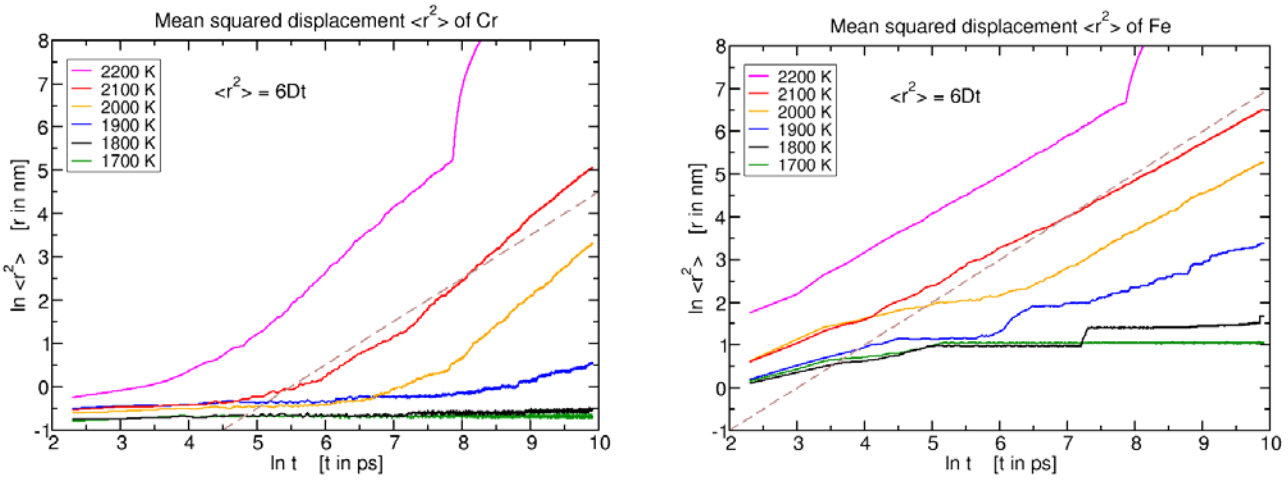

*Figure. 15. Mean squared displacement of Cr atoms (left) and Fe atoms (right) versus time, starting from the configuration shown in Figure. 14a. In three dimensions, the mean squared displacement should be $\langle \Delta r \rangle^2 = 6Dt$ as $t \to \infty$. We find here that Cr diffuses faster and Fe diffuses slower than expected, which is because of the change in concentration as time progresses. At 2200 K the system can be seen to spontaneous*ly melt around $\ln(t) \approx 8$ because of the high temper*ature.*

Figure. 15 also shows clearly that $b > 1$ for the diffusion of the Cr atoms (meaning that they diffuse faster than expected) while $b < 1$ for the Fe atoms in the system (i.e. less diffusive than expected). We can explain these results by noting that all Cr atoms start at concentration $c = 1$, and that then some of these diffuse into the Fe region. As more Cr atoms find themselves at low c, the average concentration around each Cr atom goes down, thus accelerating the increase in diffusion – resulting in super diffusive behavior as can be seen in the left panel of Figure. 15. Similarly, the average

concentration increases over time for the Fe atoms, thus leading to a reduced diffusivity. From the mean squared displacement, and assuming that $<\Delta r>^2 = 6Dt$ with $D(c)$ and $c(t)$, we can derive how the diffusion constant of each atom species changes with time, i.e. $D_{Cr}(t)$ and $D_{Fe}(t)$. This method allows us to directly obtain information about the mobility $M(c)$. Then we employ the original method of fitting the time evolution the Cr concentration starting with the configuration of a Fe-Cr-Fe "sandwich" to obtain the correct value for the interfacial energy coefficient .

The mobility can be problematic, as it is generally not a constant parameter M, but is dependent on the concentration, point defects, grain boundaries, etc. We should therefore treat it as a function of space and time, $M(\mathbf{x},t)$.

To obtain a good estimation of $M(\mathbf{x},t)$ we have developed a method to measure the mobility from molecular dynamics simulations. Molecular dynamics simulations to analyze the diffusion in crystals always take a long time to run, and therefore one must accelerate the mobility. Several ways to this is by using negative pressures, a large number of point defects, high temperatures, and a high concentration gradient. One then performs an extrapolation to higher pressures, less defects, lower temperatures, and possibly lower gradients. This approach has the additional benefit that $M(\mathbf{x},t)$ becomes dependent on defects, which is especially important when considering the effects of irradiation.

To get the impact of point-defects on the mobility, it is particularly important to quantify the number of point-defects correctly. In order to do this, we have written a program that determines the local lattice and then identifies the atoms that are not on that lattice (i.e., interstitial atoms) as well as lattice points that have no atoms assigned to it (i.e., vacancies). This program also identifies atoms that cannot be clearly assigned to one individual lattice and thus can be used to identify atoms along a grain boundary.

In line with other modules that are part of the MOOSE framework, we have decided to use an animal name for the module that we are developing in this project. The main task of the module is to take atomic data extracted from molecular dynamics simulations and use it as input for phase field simulations, and we have therefore decided to name the module "Atoms to Phase-field Evaluator" or *APE*. This module has been posted on the Internet and its website address is physics.bu.edu/ape (see Figure. 16). We plan to use this website as a platform for all documentation, and will also serve as a convenient location for people to download the program and code.

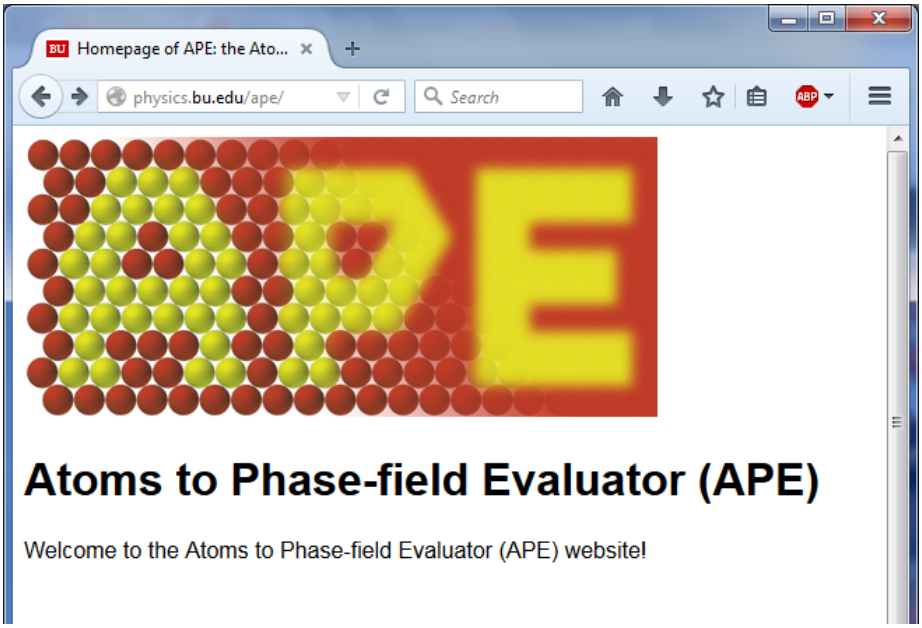

Figure. 16: Firefox displaying the APE website, via which we will make all documentation and code available to the public.

We have successfully developed an algorithm to use Molecular Dynamics data to generate the input parameters for Phase Field simulations, in particular the interfacial energy coefficient κ and the mobility $M(c)$ which depends on the Cr concentration c within the Fe matrix. This algorithm simulates a layer of 100% Cr sandwiched between two layers of 100% Fe, as this produces a large concentration gradient. The simulation is done both with Molecular Dynamics as well as with the Phase Field method, and the input parameters of the Phase Field simulation are adjusted in such a way that it exactly reproduces the output of the Molecular Dynamics simulation. Even though the Molecular Dynamics and Phase Field simulations produce exactly the same results, the Phase Field calculations are orders of magnitudes faster.

During the Molecular Dynamics simulations, in order to increase the diffusion of the Cr into the Fe matrix, we employ high temperatures and negative pressures, and add a small percentage of point defects. After successfully tweaking the Phase Field input parameters such that the output of both methods match, we then extrapolate the parameters to lower temperatures and higher pressures.
Unfortunately the Molecular Dynamics simulations require a very long time to run, and the times necessary increase rapidly as we lower the temperature. Therefore, in the past few months we have been investigating possible ways to speed up these simulations.

In order to be able to compare the Molecular Dynamics output with that of Phase Field, it is necessary to simulate a large system with many atoms, because it is important to obtain good statistics of the diffusion of the Cr atoms into the Fe matrix. However, the diffusion is dominated by the movement of the point defects, and it is therefore far more efficient to focus on the dynamics of a single defect on the lattice, instead of considering large system with a few defects and with many atoms that vibrate but do not change their lattice site.

For this reason we have started Molecular Dynamics simulations of much smaller systems with some average Cr concentration c and with only one point defect (vacancy or interstitial). These smaller systems obtain point defect statistics much more rapidly than in the original algorithm.

Of course, this leaves us with an important question: how do we translate the dynamics of the point defects into diffusion of Cr atoms in the Fe matrix? To answer this problem, we developed a method called Defect-On-Lattice (DOL) that uses the point defect dynamics as input, and produces a trajectory file similar to what regular Molecular Dynamics would produce. The main difference between the Defect-On-Lattice simulation and the Molecular Dynamics is that in the DOL simulation only the point defects move, and all other atoms are fixed to their lattice site. In addition, the Defect-On-Lattice simulation is event-based – it moves the defect to another lattice side after randomly chosen times, with those times extracted from the hoping-time distributions that were generated by the Molecular Dynamics simulations. The result is a fast, efficient simulation of the point dynamics in the lattice.

The trajectory file produced by the Defect-On-Lattice simulation can be compared to the output of the Phase Field simulation, and this way we can estimate the Phase Field input parameters.

Instead of running Molecular Dynamics simulations with only one defect, it is also possible to run simulations with two or more defects, which helps to quantify the interactions between defects. This is an important thing to measure if one wishes to study the precipitation of vacancies (the formation of cavities) and the precipitation of interstitials.

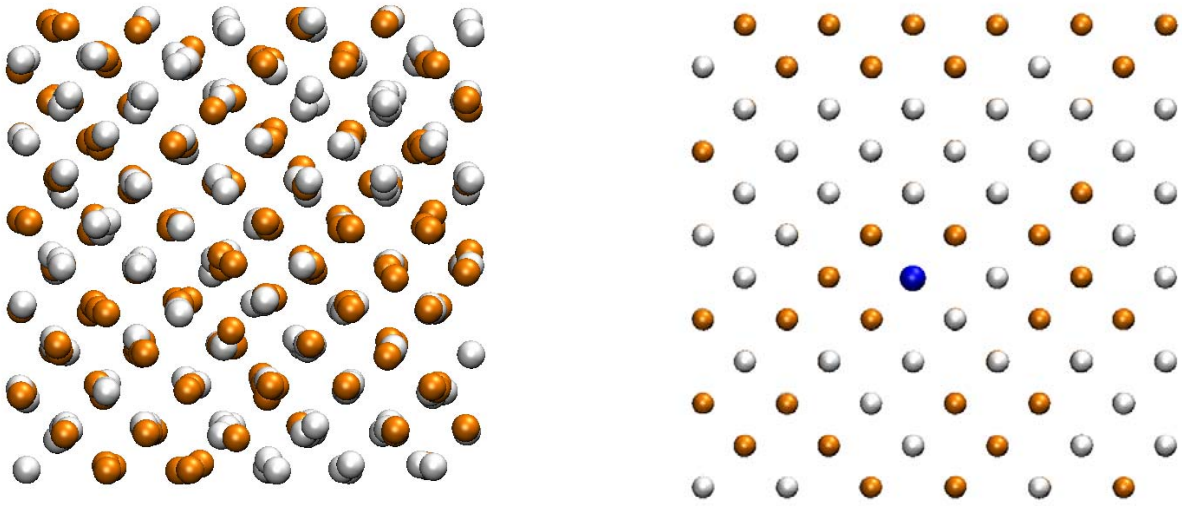

Figure. 17: (left) Snapshot of a Molecular Dynamics simulation with one vacancy. The positions of all atoms are updated in steps of typically 1 femtosecond. Cr atoms are indicated in orange and Fe atoms in white. (right) Snapshot of a Defect-On-Lattice simulation with one vacancy. Here only the atoms are fixed to their lattice site, and only the defect (represented by a blue atom) moves with steps of picoseconds to nanoseconds (depending on the temperature). Cr atoms are indicated in orange and Fe atoms in white.

Work to do

We have already established a systematic method to connect MD and PF simulation. One of the most important discoveries is that the mobility of atoms is dependent on the Cr concentration in Fe-Cr alloy. This phenomenon needs further exploration since the traditional PF method treats mobility as a constant value and significant improvement will be achieved if such assumption can be modified in PF. Moreover, the point defects and boundaries in lattice also have strong impact on the mobility of atoms,

which drives us to develop the module *APE* to locate the defects and boundaries. However, efficiency and accuracy of *APE* module is not satisfying so the module still needs further improvement. In addition, the defects interaction in lattice is so important for the mobility variation that we started to develop Defect-On-Lattice method to simulate the point dynamics of lattice. However, such development was not finished due to the tight schedule and further work is required.

References

[1] G.J. Ackland, M.I. Mendelev, D.J. Srolovitz, S. Han, and A.V. Barashev, *Journal of physics: condensed matter*, 16 (2004) S2629–S2642.

[2] Par Olsson, Janne Wallenius, Christophe Domain, Kai Nordlund, and Lorenzo Malerba, *Physical Review B*, 72 (2005) 214119.

[3] Maxie Eckert, Erik Neyts and Annemie Bogaerts, *CrystEngComm*, 11 (2009) 1597-1608.

[4] Bonny *et al.*, "Numerical prediction of thermodynamic properties of iron–chromium alloys using semi-empirical cohesive models: The state of the art", J. Nucl. Mat. **385**, 268 (2009)

[5] Caro *et al.*, "Classical Many-Body Potential for Concentrated Alloys and the Inversion of Order in Iron-Chromium Alloys", Phys. Rev. Lett. **95**, 075702 (2005)

[6] A. Caro, M. Caro, P. Klaver, B. Sadigh, E. M. Lopasso and S. G. Srinivasan, "The Computational Modeling of Alloys at the Atomic Scale: From Ab Initio and Thermodynamics to Radiation‐Induced Heterogeneous Precipitation", JOM 59, 52 (2007)

[7] Y. Li, S. Hu, L. Zhang and X. Sun, "Non‐classical nuclei and growth kinetics of Cr precipitates in FeCr alloys during ageing", Modelling Simul. Mater. Sci. Eng. 22, 025002 (2014)

[8] The Multiphysics Object‐Oriented Simulation Environment (MOOSE) framework. More information is available on http://mooseframework.org/

[9] D. Schwen, E. Martinez and A. Caro, *"On the analytic calculation of critical size for alpha prime precipitation in FeCr"*, J. Nucl. Mater. **439**, 180-184 (2013)

[10]Y. Li, S. Hu, L. Zhang and X. Sun, *"Non-classical nuclei and growth kinetics of Cr precipitates in FeCr alloys during ageing"*, Modelling Simul. Mater. Sci. Eng. **22**, 025002 (2014)

[12]B. Sadigh and P. Erhart, *"Calculation of excess free energies of precipitates via direct thermodynamic integration across phase boundaries"*, Phys. Rev. B **86**, 134204 (2012)